Journal of Power Sources 189 (2009) 676–680

Contents lists available at ScienceDirect

Journal of Power Sources

journal homepage: www.elsevier.com/locate/jpowsour

Short communication

Bulk and surface structure investigation for the positive electrodes of degraded lithium-ion cell after storage test using X-ray absorption near-edge structure measurement

Daisuke Mori, Hironori Kobayashi, Masahiro Shikano*, Hiroaki Nitani, Hiroyuki Kageyama, Shinji Koike, Hikari Sakaebe, Kuniaki Tatsumi

Research Institute for Ubiquitous Energy Devices, National Institute of Advanced Industrial Science and Technology (AIST), 1-8-31 Midorigaoka, Ikeda, Osaka 563-8577, Japan

ARTICLE INFO

Article history:
Received 31 July 2008
Received in revised form 25 August 2008
Accepted 28 August 2008
Available online 3 September 2008

Keywords:
Lithium–nickel-based oxide
Positive electrode
Power fade of lithium-ion cell
Neutron diffraction
Synchrotron radiation
XANES measurement

ABSTRACT

Cylindrical lithium-ion cells with a lithium–nickel–cobalt–aluminum oxide ($LiNi_{0.8}Co_{0.15}Al_{0.05}O_2$) and a non-graphitizable carbon (hard carbon) as the positive and negative electrodes, respectively, were degraded by the storage tests with 50% state-of-charge (SOC). The degraded cells were disassembled and positive electrodes obtained were examined. The cation distribution of lithium and nickel in the positive electrode was clarified using neutron and synchrotron X-ray diffraction measurements. The degree of lithium and nickel disordering varied with the storage condition. X-ray absorption near-edge structure (XANES) analysis demonstrated that the structural change was mainly located near the surface of the positive electrode and the valence state of Ni and Co ions did not change with the storage test. The disordering of the cations near the surface was closely related to the power fade of the cell. The storage condition is an important factor in the power fade of lithium-ion cells.

1. Introduction

Lithium batteries have attracted much attention as a key technology for hybrid electric vehicles (HEV), plug-in HEV and pure electric vehicles (EV) because of an interest in reducing emission of carbon dioxide and use of alternative energy sources. These batteries require high specific power and long life over 10 years in addition to conventional demands for portable devices. The achievement of long life for the lithium-ion cell is necessary to suppress the degradation due to the cycle and storage. Therefore, much effort has been devoted to understand the degradation mechanism such as the capacity and power fade of the lithium-ion cell.

Lithium–nickel–cobalt-based oxide with layered rocksalt type structure was investigated as one of the main candidates of the positive electrode for HEV and EV systems [1]. The interfacial resistance of the positive electrode was found as the cause of the cell impedance rise after accelerated calendar life and cycle life tests [2]. Then, the surface structure of the positive electrode and electrode/electrolyte interface were extensively investigated [3–13]. After cycle tests the surface structure change of the electrode was detected by X-ray absorption near-edge structure (XANES) analysis, high-resolution transmission electron microscopy (HRTEM) and electron energy loss spectroscopy (EELS) [3]. The surface structure change to the NiO-like structure resulted from the loss of cation ordering between Ni and Li in layered rocksalt structure. X-ray photoemission spectroscopy (XPS) revealed that a mixture of organic species such as polycarbonate, LiF, Li_xPF_y-type and $Li_xPF_yO_z$-type compounds were formed on the surface of the positive electrodes with various test temperatures, durations and state-of-charge (SOC) [4].

The variants in the vicinity of positive electrode surface were considered the deterioration factor in the performance of currently lithium-ion cell. However, it is difficult to say that the degraded mechanism of the lithium-ion cell has been understood sufficiently. The electrochemical property of lithium-ion cell varies with a cell configuration and the cycle condition. The characteristic of the positive electrode is also affected by SOC. Furthermore, the charge–discharge patterns required in plug-in HEV and EV are different from the conventional charge–discharge condition. Previously, we have conducted the combination study for the same lot of samples degraded by pulse cycle test of 50,000 times at various temperatures to obtain a systematic insight about the deterioration mechanism of the lithium-ion cell. XANES analysis [5], hard X-ray photoemission spectroscopy (HX-PES) [6], Fourier transform infrared spectroscopy (FT-IR) [7] and glow discharge optical emission spectrometry (GD-OES) [8] were performed to investigate the

* Corresponding author. Tel.: +81 72 751 7932; fax: +81 72 751 9609.
E-mail address: shikano.masahiro@aist.go.jp (M. Shikano).

0378-7753/$ – see front matter © 2008 Elsevier B.V. All rights reserved.
doi:10.1016/j.jpowsour.2008.08.073

inside and outside near the surface of the degraded positive electrode. The positive electrode had the lithium deficient cubic phase near the surface, while the layered structure was retained in the bulk after the pulsed cycle test [5]. Li_2CO_3, hydrocarbons, $ROCO_2Li$, polycarbonate-type compounds and LiF were observed on the positive electrode and the amount of carbonates depended on SOC [6]. Based on these results we proposed a schematic view to describe the changes taking place near the surface of the positive electrode during the cycle test. However, the deterioration by the cycle test might include some influences of the storage period and temperature, since a large number of cycle tests take long time. In order to comprehend the details of the deterioration mechanism of the lithium-ion cell, the separation of the factor involved in the storage condition is necessary. In this study, $LiNi_{0.8}Co_{0.15}Al_{0.05}O_2$ positive electrodes obtained from the cells, which had undergone the power fade by the storage tests, were examined by neutron diffraction (ND) and synchrotron X-ray diffraction (XRD) measurements and XANES analysis. The relationship between the power fade and the surface structure of the positive electrode will be discussed.

2. Experimental

18650 type cylindrical cells of capacity 380 mAh were fabricated for this study, which were designed to have a rate capability of more than 10 C. The cells were constructed from pressed double-side coated electrodes using a high-power design. The positive electrode was comprised $LiNi_{0.8}Co_{0.15}Al_{0.05}O_2$ (NCA-01, Toda Kogyo Corp.), acetylene black (HS-100, DENKA) and poly(vinylidene difluoride) (PVdF) binder (KF1320, Kureha Corp.). The negative electrode consisted of non-graphitizable carbon (hard carbon) (Carbotron® PS(F), Kureha Corp.) and PVdF binder (KF1120, Kureha Corp.). 1 M $LiPF_6$ in propylene carbonate (PC)/diethyl carbonate (DEC) with the volume ratio of 1:1 was used as the electrolyte. The cells were degraded by the storage test at 40 °C and 60 °C after conditioning and controlling at 50% SOC. The dc resistance was calculated from the slope of $-\Delta V/\Delta I$ as previously reported [5]. The test cells were controlled at 50% SOC and then disassembled immediately after the predefined test period. The obtained electrodes were washed by dimethyl carbonate (DMC) and then dried in vacuum.

Time-of-flight neutron powder diffraction data were collected on the Special Environment Powder Diffractometer (SEPD) at the Intense Pulsed Neutron Source (IPNS) in the Argonne National Laboratory (Proposal No. 5126). The collected data using 90° detector banks were used for structural refinements. Synchrotron XRD data were taken on a Debye–Scherrer type powder diffractometer with an imaging-plate (IP) type detector installed in the beamline BL02B2 at SPring-8 with the approval of the Japan Synchrotron Radiation Research Institute (Proposal No. 2006A1016). The wavelength of the incident synchrotron radiation was fixed at 0.5011 Å. The structural parameters were refined by the Rietveld analysis using the program GSAS+EXPGUI [14,15] for the neutron data and the program RIETAN2000 [16] for the synchrotron X-ray data.

The Ni and Co $L_{II,III}$-edge and O K-edge XANES spectra were measured on the beamline BL4B of the UVSOR Facility with the approval of the Institute of Molecular Science (Proposal No. 19-225) in the total electron yield (TEY) mode and on the beamline BL27SU of the SPring-8 (Proposal No. 2007A2046) in the TEY and fluorescence yield (FY) modes.

3. Results and discussion

3.1. Performance of the test cells

The storage test was carried out at 40 °C and 60 °C after the cells were controlled at 50% SOC. The storage period dependences of the relative specific power for the test cell are shown in Fig. 1. The relative specific power of the degraded cell showed a larger decrease at 60 °C than at 40 °C with the storage period. The specific power of the cell stored at 60 °C for 12 weeks decreased to 0.81, while that of the cell stored at 40 °C showed a slight decrease to 0.98. The power fade of the cell also depended on the storage period. The specific power of the cell stored for 96 weeks decreased to 0.87 at 40 °C and 0.57 at 60 °C. The storage tests demonstrated that the power fade of the cells proceeded depending on the temperature and periods without charge–discharge cycles. Meanwhile, the power fade behavior of the storage test cell was similar to that of the pulsed cycle test cell [5]. It is considered that the deterioration of the cells depending on the storage conditions contributed to the power fade of the cell degraded by the pulse cycle test. The relationship between storage conditions and other cell characteristic such as capacity and ac resistance will be discussed elsewhere [17].

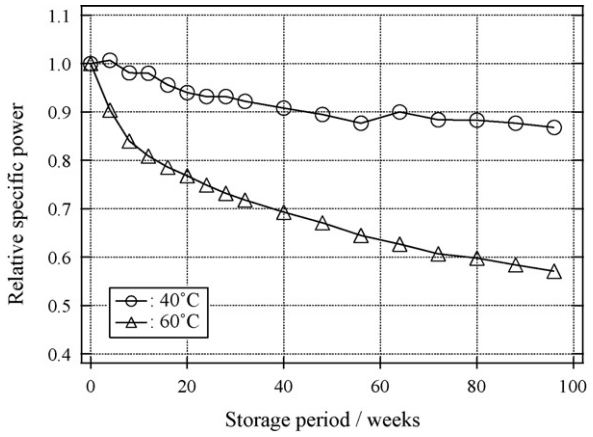

Fig. 1. Storage period dependence of relative specific power for the test cell.

3.2. Neutron and synchrotron X-ray Rietveld analysis

ND measurement is useful to investigate the structure of lithium containing materials [18–20], since the scattering length is independent of the atomic number. ND measurements were performed for the positive electrode before and after the storage test for 96 weeks at each temperature. Synchrotron XRD measurements were performed for the positive electrode before and after the storage test for 12 and 96 weeks at each temperature. No significant peak broadening and no additional peaks depending on the degradation were observed in the ND and XRD patterns obtained, indicating that the bulk structure were essentially unchanged after the storage test. The structure refinements were carried out using layered rocksalt type structure model with space group $R\bar{3}m$ (A-166-1), Li1/Ni1 at 3a site (0, 0, 0), Li2/Ni2/Co/Al at 3b site (0, 0, 0.5) and O at 6c site $(0, 0, z)$ with $z \approx 0.24$. The occupation parameters of Co and Al at 3b site were fixed at the nominal composition. The sum of occupation parameters of Ni being over two sites was constrained at the nominal value. The occupation parameter of Li at 3b site was constrained by the Ni at 3b site as the total occupation parameter at 3b site was unity. The isotropic atomic displacement parameters of all atoms and the occupation parameter of Li at 3a site were refined using the ND data. These parameters of the samples stored for 12 weeks at each temperature were fixed at the refined values of the samples stored for 96 weeks at each temperature. All samples were confirmed that both of lithium and nickel were located at 3a and 3b sites by the refinements of the ND and XRD data. Final cation distribution was determined using the XRD data. The refinement results of the sample stored at 40 °C for 96 weeks are summarized

Table 1
Structural parameters for the sample stored at 40 °C for 96 weeks

Atom	Site	g	x	y	z	U (Å^3)
Li(1)	3a	0.33(2)[a]	0	0	0	0.018(9)[a]
Ni(1)	3a	0.0125(5)	0	0	0	0.018
Ni(2)	3b	0.7865	0	0	0.5	0.0070(7)[a]
Li(2)	3b	0.0125	0	0	0.5	0.0070
Co	3b	0.146	0	0	0.5	0.0070
Al	3b	0.055	0	0	0.5	0.0070
O	6c	1	0	0	0.23520(7)	0.0084(7)[a]

$R\bar{3}m$, a = 2.82299(4) Å, c = 14.4715(4) Å, R_{wp} = 2.93%, R_p = 2.19%, R_R = 6.68%, R_e = 2.65%, R_I = 1.46%, R_F = 0.94%, $S = R_{wp}/R_e$ = 1.11.
[a] Determined by the ND data (R_p = 4.60%).

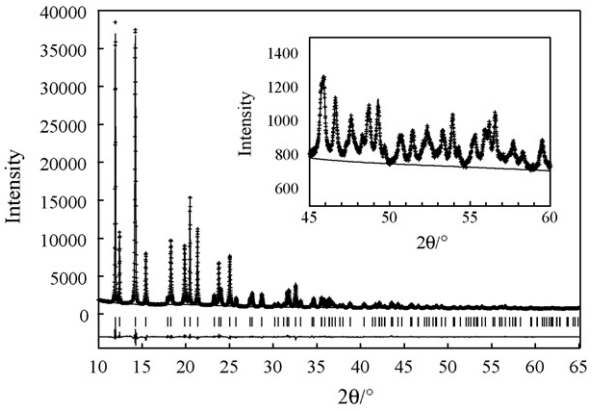

Fig. 2. Observed (+), calculated (solid black line) and difference (solid gray line) plots for synchrotron X-ray Rietveld refinement for the sample stored at 40 °C for 96 weeks. The inset shows Rietveld refinement plots in a 2θ region from 45° to 60°.

in Table 1 and shown in Fig. 2. Fig. 3 shows the relative specific power dependence of the occupation parameter of Ni at 3a site. The cation disordering of the degraded cells increased as the relative specific power decreased. Therefore, the degree of the disordering of lithium and nickel ions would closely correlate with the degradation of the cell. The cation ordering involved in the power fade by the cycle and pulse cycle degradation tests was reported for the cell

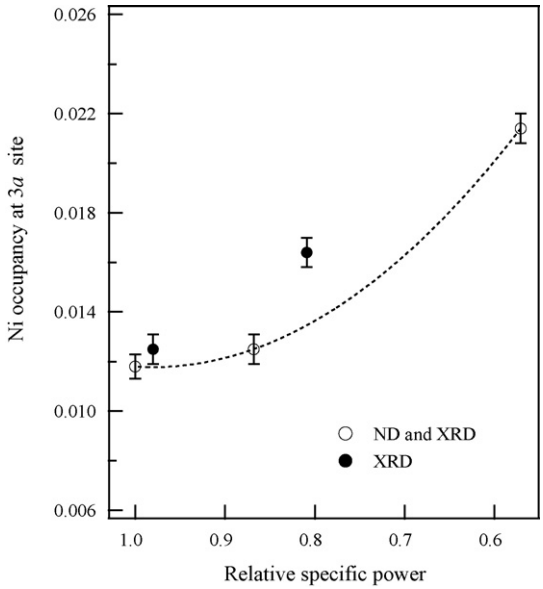

Fig. 3. Relative specific power dependence of Ni occupancy at 3a site of the positive electrode before and after storage test.

using the lithium–nickel–cobalt-based oxide as the positive electrode [3,5]. Our result corresponding to them indicates that the influence of storage conditions in the degradation of the cell is not negligible to consider the degradation mechanism during the cycle test for long time.

3.3. XANES analysis

In order to investigate the surface of the $LiNi_{0.8}Co_{0.15}Al_{0.05}O_2$ positive electrode, Ni and Co $L_{II,III}$-edge and O K-edge XANES spectra were collected in the TEY mode using soft X-ray. XANES spectra measured in the TEY mode provide the information near the surface. Fig. 4 shows Ni and Co $L_{II,III}$-edge XANES spectra of the positive electrodes before and after the storage test. No significant change of spectrum shape depending on the deterioration state was observed in the Ni and Co spectra. It indicates that the surroundings of the nickel and cobalt did not vary with the storage conditions. No significant peak shifts of the Ni and Co L-edge spectra were observed either, indicating that the Ni and Co valences were invariant during the storage test. These results are different from the previous results of the XANES study for the positive electrode degraded by the cycle test that Ni and Co ions in divalent state were observed on the surface with the deterioration [3].

Fig. 5 shows O K-edge XANES spectra of the positive electrodes before and after the storage test measured in the TEY mode. Three peaks were observed in the spectra for all samples. The peaks around 533.5 eV derived from Li_2CO_3 [5] are excluded from the following discussions. The intensity of the peak observed around 528.2 eV decreased and that around 531.5 eV increased depending on the storage period and temperature, which indicates that the surroundings of oxygen changed with the deterioration of the cell. The peaks observed around 528 eV and 531.5 eV correspond to oxygen originating from the layered structure and the disordered structure, respectively [5]. Therefore, the loss of cation ordering in the layered structure was interpreted to proceed with the degradation of the cell. Fig. 6 shows the O K-edge spectra measured in the TEY and FY modes of the positive electrodes before and after stored for 96 weeks at 60 °C. XANES spectra measured in the FY mode provide the information of the bulk structure. The difference in the spectrum shape between the sample before and after the storage test was clearly seen in the TEY mode. The peak intensity around 528 eV decreased, while the peak intensity around 531.5 eV increased with the degradation of the cell. However, no significant difference in the spectra shape between the positive electrodes before and after stored for 96 weeks at 60 °C was observed in the FY mode. Therefore, the degraded positive electrode was confirmed that the disordering of cation arrangement was located near the surface and the bulk structure was independent of the storage condition.

3.4. Discussions

In the present study, the power fade of lithium-ion cell was shown in the storage test with 50% SOC. The cation disordering in the degraded electrodes was detected by the ND and synchrotron XRD analysis as the average information of the surface and bulk. The obtained XANES spectra in the TEY mode indicated that the surroundings of oxygen varied with the degradation of the cell. This corresponds to the results of ND and synchrotron XRD measurements. Furthermore, the disorder phase was clarified to be near the surface of the positive electrode by the XANES measurements in the TEY and FY modes. Therefore, the power fade of the cell with the storage test was considered to correlate with the disordered phase near the surface of the positive electrode. The structural change from layered structure to cubic structure accompanied with the

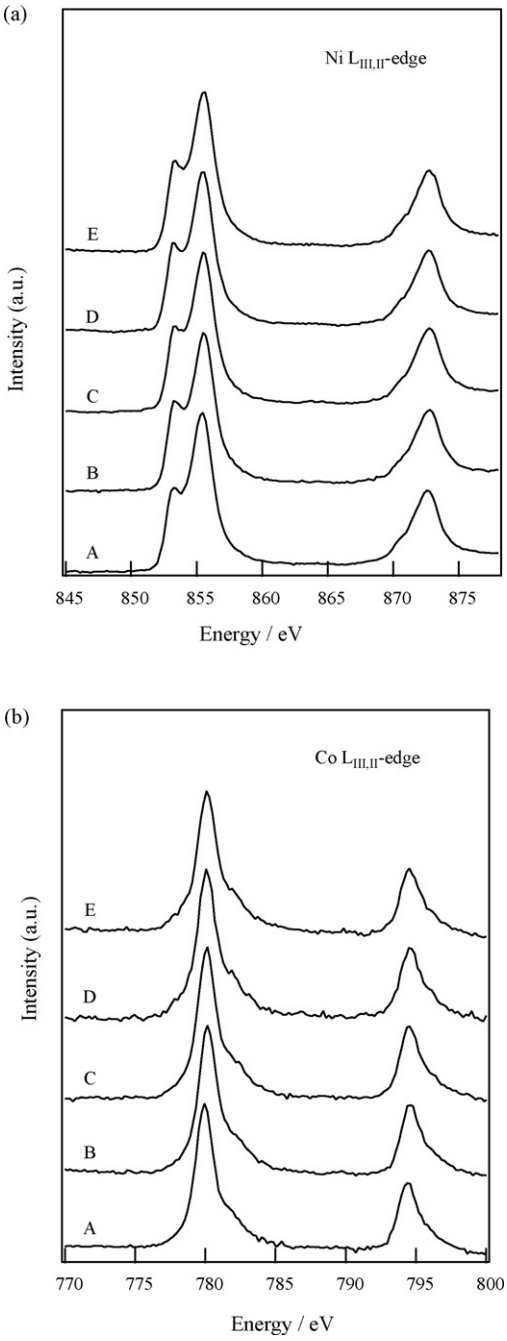

Fig. 4. Ni (a) and Co (b) $L_{III,II}$-edge XANES spectra of the positive electrode before and after storage test. Sample A: before test; sample B: 40 °C, 12 weeks; sample C: 40 °C, 96 weeks; sample D: 60 °C, 12 weeks and sample E: 60 °C, 96 weeks.

loss of cation ordering for the $LiNi_{0.8}Co_{0.2}O_2$ electrode degraded by the cycle and pulse cycle tests [3,5]. The cation disordering detected in this study corresponds to the disordered cubic phase previously reported [5,6]. Therefore, the storage condition is highly involved in the deterioration by the pulsed cycle test.

The reduction of Ni ion to divalent state was observed in previous EELS study for the positive electrode degraded by the cycle test [3]. No decrease of the valence of Ni and Co ions was observed by the storage test with 50% SOC in our Ni and Co $L_{III,II}$-edge XANES measurements. The difference in the valence state of the Ni ion is not conflictive because the Ni^{4+} ion could transform to Ni^{2+} ion at high SOC state for the lithium–nickel-based oxides. However,

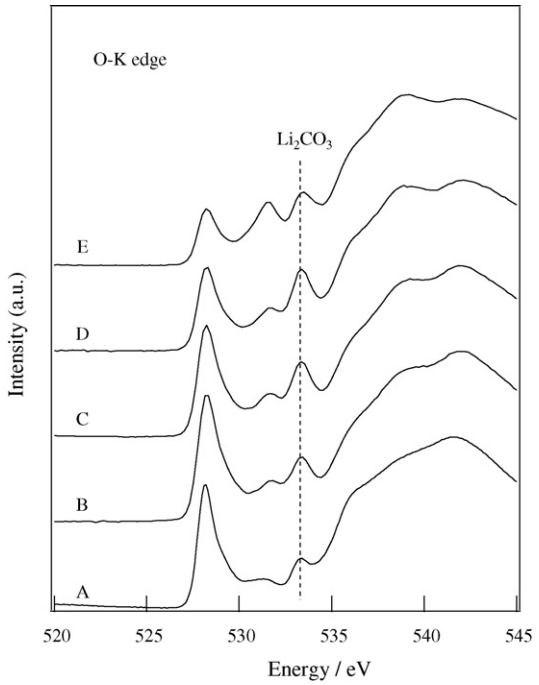

Fig. 5. O K-edge XANES spectra of the positive electrode before and after storage test. Sample A: before test; sample B: 40 °C, 12 weeks; sample C: 40 °C, 96 weeks; sample D: 60 °C, 12 weeks and sample E: 60 °C, 96 weeks.

the power fade of the cell was observed in both the storage and cycle degradation tests. Therefore, the transformation of Ni^{4+} to Ni^{2+} ion is not so important factor for the power fade of the cell. The cation disordering closely correlates with the power fade of the cell with lithium–nickel-based oxides as we previously reported [5,6]. The cation disordering might be attributed to not only electrochemical lithium (de-)intercalation but also thermal motion and

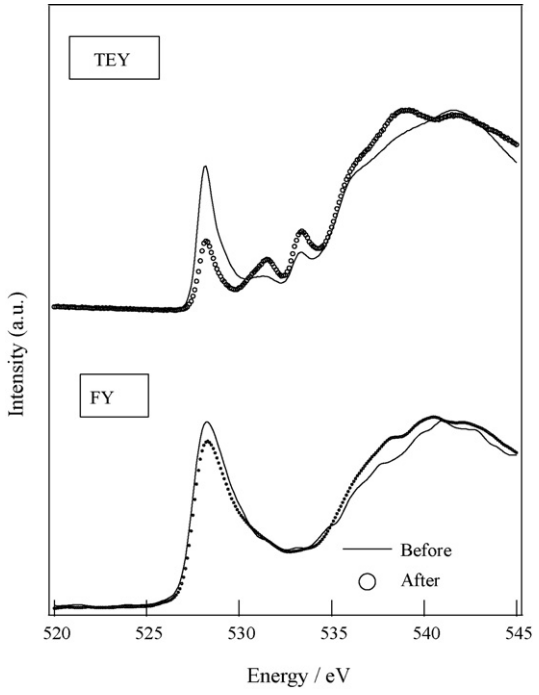

Fig. 6. O K-edge XANES spectra of the positive electrode before and after storage test at 60 °C for 96 weeks measured in both TEY and FY modes.

ion exchange at the interface of electrode/electrolyte. The lithium ion in the electrode and the electrolyte would reciprocate continually at the interface, even if the cell voltage is kept constant. The lithium migration near the surface and thermal motion of the nickel might lead to the cation disordering without the electrochemical lithium intercalation. Consequently, the cation disordering would be located near the surface of the electrode.

Previously, we reported that the disordered cubic phase near the surface of the positive electrode and the surface film consisting of the Li_2CO_3, LiF and carbonates on the electrode were the factors of power fade of the cell degraded by the pulse cycle tests [5,6]. The formation and amounts of surface film of the positive electrode was affected by the cell voltage [21], SOC [6] and/or lithium de-intercalation [9]. The surface analysis of the degraded electrode by the storage test is necessary to draw more precise power fade mechanism of the lithium-ion cells in the future.

4. Conclusion

The positive electrode obtained from the degradation cells by the storage test with 50% SOC was examined. The power fade of the lithium-ion cells was demonstrated to correlate with the cation disordering of the positive electrode using ND and synchrotron XRD measurements and XANES analysis. The XANES analysis also revealed that the valence of Ni ion did not vary with the storage condition and the structural change from the layered structure to the disordered cubic structure was located near the surface of the positive electrode. The cation disordering depending on the storage period and temperature proceeded without electrochemical lithium intercalation. To understand the degradation mechanism of the lithium-ion cells the storage condition is an important factor as well as the cycle condition of the test cell.

Acknowledgements

This work was supported by “the Lithium-ion and Excellent Advanced Batteries Development (Li-EAD) project” of the New Energy and Industrial Technology Development Organization (NEDO) in Japan. ND measurements were supported by the High Energy Accelerator Research Organization (KEK). XANES measurements at SPring-8 were performed as a Nanotechnology Support Project of Japan’s Ministry of Education, Culture, Sports, Science and Technology.

References

[1] K. Amine, J. Liu, ITE Lett. 1 (2000) 59–63.
[2] K. Amine, C.H. Chen, J. Liu, M. Hammond, A. Jansen, D. Dees, I. Bloom, D. Vissers, G. Henriksen, J. Power Sources 97–98 (2001) 684–687.
[3] D.P. Abraham, R.D. Twesten, M. Balasubramanian, J. Kropf, D. Fischer, J. McBreen, I. Petrov, K. Amine, J. Electrochem. Soc. 150 (2003) A1450–A1456.
[4] A.M. Andersson, D.P. Abraham, R. Haasch, S. MacLaren, J. Liu, K. Amine, J. Electrochem. Soc. 149 (2002) A1358–A1369.
[5] H. Kobayashi, M. Shikano, S. Koike, H. Sakaebe, K. Tatsumi, J. Power Sources 174 (2007) 380–386.
[6] M. Shikano, H. Kobayashi, S. Koike, H. Sakaebe, E. Ikenaga, K. Kobayashi, K. Tatsumi, J. Power Sources 174 (2007) 795–799.
[7] M.K. Rahman, Y. Saito, J. Power Sources 174 (2007) 889–894.
[8] Y. Saito, M.K. Rahman, J. Power Sources 174 (2007) 877–882.
[9] M. Hirayama, K. Sakamoto, T. Hiraide, D. Mori, A. Yamada, R. Kanno, N. Sonoyama, K. Tamura, J. Mizuki, Electrochim. Acta 53 (2007) 871–881.
[10] H. Kobayashi, S. Emura, Y. Arachi, K. Tatsumi, J. Power Sources 174 (2007) 774–778.
[11] K. Edstrom, T. Gustafsson, J.O. Thomas, Electrochim. Acta 50 (2004) 397–403.
[12] T. Nonaka, C. Okuda, Y. Seno, Y. Kondo, K. Koumoto, Y. Ukyo, J. Electrochem. Soc. 154 (2007) A353–A358.
[13] M. Balasubramanian, H.S. Lee, X. Sun, X.Q. Yang, A.R. Moodenbaugh, J. McBreen, D.A. Fischer, Z. Fu, Electrochem. Solid State Lett. 5 (2002) A22–A25.
[14] A.C. Larson, R.B. Von Dreele, Los Alamos National Laboratory Report LAUR, 2000, 86-748.
[15] B.H. Toby, J. Appl. Crystallogr. 34 (2001) 210–213.
[16] F. Izumi, T. Ikeda, Mater. Sci. Forum 321–324 (2000) 198–205.
[17] M. Shikano, H. Sakaebe, H. Kobayashi, S. Koike, H. Nitani, D. Mori, Y. Saito, K. Tatsumi, in preparation.
[18] H. Kobayashi, H. Sakaebe, H. Kageyama, K. Tatsumi, Y. Arachi, T. Kamiyama, J. Mater. Chem. 13 (2003) 590–595.
[19] A. Hirano, R. Kanno, Y. Kawamoto, Y. Takeda, K. Yamaura, M. Takano, K. Ohyama, M. Ohashi, Y. Yamaguchi, Solid State Ionics 78 (1995) 123–131.
[20] H. Kobayashi, Y. Arachi, S. Emura, H. Kageyama, K. Tatsumi, T. Kamiyama, J. Power Sources 146 (2005) 640–644.
[21] S.W. Song, G.V. Zhuang, P.N. Ross, J. Electrochem. Soc. 151 (2004) A1162–A1167.